Kenneth J. Waldron
Department of Mechanical Engineering,
Stanford University,
Stanford, CA 94305

J. Estremera
Industrial Automation Institute-CSIC,
28500 La Poveda,
Madrid, Spain

Paul J. Csonka
Department of Mechanical Engineering,
Stanford University,
Stanford, CA 94305

S. P. N. Singh
Australian Centre for Field Robotics,
Rose St. Bldg. J04,
The University of Sydney,
NSW 2006, Australia

Analyzing Bounding and Galloping Using Simple Models

This paper focuses on modeling the gait characteristics of a quadrupedal gallop. There have been a number of studies of the mechanics of the stance phase in which a foot is in contact with the ground. We seek to put these studies in the context of the stride, or overall motion cycle. The model used is theoretical, and is kept simple in the interest of transparency. It is compared to empirical data from observations of animals, and to data from experiments with robots such as our KOLT machine, and results from sophisticated simulation studies. Modeling of the energy loss inherent in the interaction between the system and the environment plays a key role in the study. Results include the discovery of a hidden symmetry in the gait pattern, usually regarded as being completely asymmetrical. Another result demonstrates that the velocities with which the two front feet impact and leave the ground are different, and similarly for the rear feet. The velocities of the foot pairs mirror each other. This is consistent with empirical observation, but is at variance with the assumption used almost universally when modeling stance. A further result elicits the importance of the pitch moment of inertia and other effects that make the mammalian architecture, in which the center of mass is closer to the shoulders than to the hips, beneficial.. [DOI: 10.1115/1.2959095]

Introduction

Quadrupedal animals use a variety of gaits (foot timing programs) for dynamic locomotion. These include the trot, in which the diagonally opposite feet are placed, and lifted, simultaneously; the pace, in which the feet on the same side of the body are used in synchrony; and the bound, in which the two front feet are used simultaneously, as are the two rear feet. Another variant is the pronk, in which the animal leaps off all four feet simultaneously. The most difficult gait to model dynamically is the gallop. A gallop is intrinsically different from the other dynamic gaits in that the feet are used individually and the footfall timing lacks any apparent symmetry. A further mystery is the use of two different types of gallop: the transverse gallop in which the left-right sequence where the back feet are placed is the same as that at the front, and the rotary gallop in which the sequence at the back feet is the reverse of that at the front (Figs. 7 and 9). There are good runners that use each of these gaits: horses, and most antelopes prefer transverse gallops. Cheetahs, other cats, and some dogs use rotary gallops. As is discussed below, there are significant dynamic differences between the two varieties of gallop. A study of dynamic quadrupedal locomotion produces the conclusion that all degrees of freedom of system motion are coupled [1].

In the present paper, we attempt to understand the important mechanical features of bounding and galloping using arguments based on simple models. Bounding is used as a starting point for developing models of galloping. In practice, mammals switch easily from a bound to a gallop, and vice versa. For example, when it is necessary to leap across a large obstacle, an animal will shift from a gallop to a bound, resuming the gallop after the leap is completed. Krasny and Orin [2] obtained a similar behavior in a dynamic model that evolved its gait via an evolutionary algorithm.

Simplifying the mechanics, of course, means that some effects and subtle interactions are lost, and it is possible to come to incorrect conclusions. Numerical results are suspect. Nevertheless, simple models can lead to deep insights. It is the insights that we are seeking here. Accurate modeling in simulation can then produce reliable quantitative results.

Contributed by the Mechanisms and Robotics Committee for publication in the JOURNAL OF MECHANISMS AND ROBOTICS. Manuscript received April 4, 2008; final manuscript received June 22, 2008; published online July 30, 2008. Review conducted by Frank C. Park. Paper presented at the CLAWAR 2007.

Experimental data against which the results can be validated are quite sparse. However, a recent paper does provide data from force plate experiments with galloping dogs against which some of the more important assumptions can be validated [3]. Other results can be compared to simulation results such as those of Ref. [2] cited above.

Front-Rear Force Distribution

It is notable that almost all mammals are built with their center of mass closer to the shoulders than to the hips. In Ref. [4] the center of mass of a large dog is located at 65% of the shoulder-hip distance ahead of the hips. This is fairly consistent with Ref. [5] where it was found that dogs of various breeds support 61% of their weight on the front legs. In both these references the measurement was done statically. In Ref. [3] the ratio of the weight borne on the front legs to that borne on the rear was measured dynamically when galloping (for six dogs). The calculated value is 57% of the weight being carried by the front legs. This is a result of the head and neck being cantilevered forward of the shoulders in running posture (Figs. 7 and 9) and also the forward position of the rib cage and the muscles anchored to it. The difference between the static and dynamically measured values is explained by dynamic load transfer, with an inertia force applied at the center of mass when the system is being accelerated by the rear legs.

Experimental evidence [3,6–8] indicates that when running, most mammals place the forefeet well ahead of the vertical projection of the shoulder. The shoulder pole vaults over the leg, thereby converting some horizontal kinetic energy into vertical kinetic energy and helping to generate the vertical component of the leg thrust. The net impulse from the front leg winds up having a small rearward component in the horizontal direction, as shown in Fig. 1. The net horizontal thrust at the front legs for galloping dogs was found to be essentially zero [3].

In contrast, the rear legs are placed only a little ahead of the vertical projections of the hips, or possibly even further back, and generate an impulse that is strongly inclined in the forward direction [3]. The horizontal component overcomes the braking effect of the front legs and provides enough forward thrust to overcome the effective drag on the system. The vertical component is smaller than that at the front legs but is sufficient to provide moment equilibrium, as ensured by the concurrency condition.

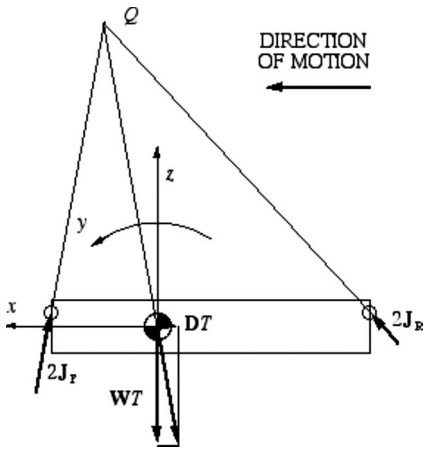

Fig. 1 Impulsive equilibrium over the duration of a stride for a bound. W is the weight of the system, and D is the drag. *T* is the stride duration. $2J_F$ is the net impulse imparted by the front feet, and $2J_R$ is that imparted by the rear feet.

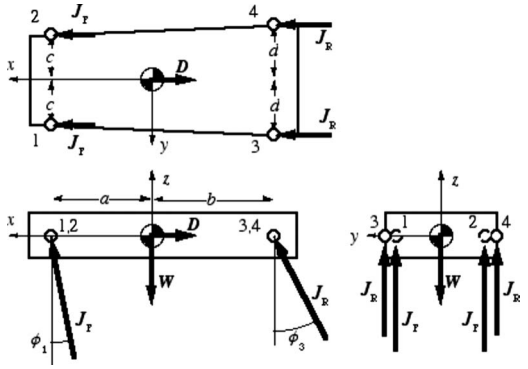

Fig. 2 Free body diagram. The center of mass is assumed to be coplanar with the shoulder and hip joints. It can be argued that the location of the center of mass a small distance above or below the plane of the joints makes little difference to the dynamics. The shoulder and hip joints are assumed to be pairs of intersecting revolutes that are, respectively, parallel to the *x* axis of the body and orthogonal to the plane of the leg. The body reference frame is centered on the center of mass and aligned as shown. The principal axes of inertia are assumed to coincide with the *x*, *y*, and *z* axes.

Let us first consider a bound. Here the front feet touch down simultaneously, as do the rear feet. External forces, other than gravity, can only be applied to the system when the feet are on the ground. When the system is in the air, the only force acting is gravity, the center of mass follows a ballistic trajectory, and the angular momentum of the system is conserved.

We consider only stably repetitive motion in which the system returns to exactly the same state after one complete motion cycle or stride. We also assume that angular motions of the body are small and that the forces imparted to the body by the legs act along the leg axes from the point of contact with the ground to the hip/shoulder center. This is actually equivalent to the assumption of massless legs. However, it is a quite good approximation for fast running even if the legs have significant inertia [9].

It is assumed that small angle approximations can be applied to all three of the attitude axes. This is certainly not valid for the pitch angle, θ_y, in a deep bound, as would be used to leap over an obstacle. However, for relatively shallow bounds like those used for rapid locomotion by some small animals, it is a reasonable approximation. Certainly it is reasonable when galloping, which has the effect of minimizing pitch rotations. Significant angular magnitudes may also be observed in the roll angle, θ_x, in animals that use rotary gallops with long stride periods. Runners of this type do seem to have special adaptations to cope with large roll angles. We believe that a small angle approximation can be used in roll for most bounding and galloping systems.

The mass of the legs is neglected, and the moment of inertia of the system about its mass center is assumed to be constant. These are probably the least defensible of the simplifying assumptions made here. As was shown by Schmiedeler et al. [4], the leg masses and variations in the positions of the legs result in significant variations in the pitch moment of inertia, I_y. Nevertheless, in the interests of transparency, we choose to regard I_y as constant.

We choose to work in the impulse-momentum domain, allowing us to consider an impulse balance over the entire stride period, *T*. We also work in a reference frame fixed to the body. This does not imply that we regard the stance period as being instantaneous. Rather, we integrate the contact force during stance with respect to time. This is analogous to replacing a spatially distributed force system by its resultant. In that case we integrate over the area of action of the force system. In the present case, the force is temporally distributed, and we use the product of its time average with the duration of action. We will discuss the effects of replacing each contact force by its impulse in some detail below when interpreting the results of the theoretical models based on these assumptions.

If the net impulse imparted to the system by the front feet is $2\mathbf{J}_F$ and that imparted by the rear feet is $2\mathbf{J}_R$, and **W** and **D** are the weight of the system and the drag, respectively, the system becomes a three-force system. Therefore the lines of action of the front and rear impulses must be concurrent with that of the impulse of the resultant of the weight and drag, as shown in Figs. 1 and 2.

The equivalent dynamic equilibrium equations are

$$2\mathbf{J}_{Fx} + 2\mathbf{J}_{Rx} = \mathbf{D}T \tag{1}$$

$$2\mathbf{J}_{Fz} + 2\mathbf{J}_{Rz} = \mathbf{W}T \tag{2}$$

$$a\mathbf{J}_{Fz} = b\mathbf{J}_{Rz} \tag{3}$$

It is perfectly possible to generate appropriate leg impulses for running regardless of the location of the center of mass. Why then are mammals consistently constructed with their centers of mass forward of the midpoint of the body?

The effect of the near vertical thrust of the front legs is to pitch the system back when viewed in the world reference frame. This allows the rear legs to contact the ground in a more nearly vertical position than they would have done without the effect of the front legs. This, in turn, increases the horizontal component that can be generated by the rear feet without slipping. The rear legs are free to extend to their limit in order to generate as much thrust as possible without any risk of interference with the fronts,

Conversely, if the system were constructed so that $a > b$, the effect of the relatively vertical impulse received from the rear legs would be to pitch the system forward, resulting in the front legs acting at a very flat angle and making it difficult for them to generate much thrust without slipping. Further, for normal body proportions, the rear feet would need to be placed well in front of the front feet with front and rear legs overlapping substantially. This might not be a problem in straight-line locomotion, but it would certainly carry a penalty in reduced maneuverability, which could be fatal in hunter-prey interactions.

So far we have talked only in the context of the bound. If the front and rear legs are split out as in a gallop, it does not change the picture as seen from the body reference frame, as long as the corresponding left and right legs produce identical impulses, as seen from the body reference frame.

It is attractive to assume that the left and right legs of a pair generate identical impulses since they are constructed identically. The force plate data [3] indicate that although there are differ-

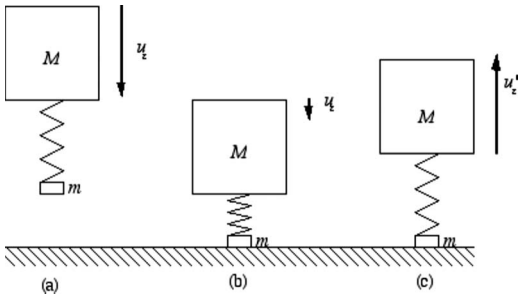

Fig. 3 Dynamic effect of a foot, mass *m*, connected to the remainder of the system *M* by a spring. The energy lost each stance is $mv_z^2/2$, where v_z is the vertical component of system velocity.

ences between the magnitudes of the force components and in the durations of the stances of the legs of each pair, the resultant impulses of each lateral pair of legs are very nearly identical, supporting the assumption. Their data also indicate that the impulse from a leg has no significant lateral component, consistent with the representation of Fig. 2.

Impact Energy

It is notable that animals can run over diverse surfaces without any noticeable effect on their gait and at very nearly the same speed. This seems anomalous since the coefficient of restitution between the foot and the ground must vary considerably and unpredictably. The reason for this capability is very simple when one considers the way the foot works when running.

Consider the system shown in Fig. 3. We model the system as having only one leg in contact with the ground and consisting of a small mass, m, representing the foot, connected to a large mass, M, representing the rest of the system by a spring. Initially the foot is at rest relative to the rest of the system with the spring at its natural length. The whole assemblage descends with velocity u. When the foot strikes the ground, it does not rebound because the mass, M, compresses the spring, and the spring force holds the foot down. Eventually M is propelled upward again by the spring, and energy is added by an actuator assisting the spring (not shown in the figure). In order for the center of mass of the entire system to have the same velocity u but in the upward direction when the foot is about to leave the ground, the velocity of the center of mass of M must be

$$u' = \frac{m+M}{M}u \tag{4}$$

The energy that the foot had when it descended ($mu^2/2$) is lost and must be replaced by the actuator. Because m is very much smaller than M, this energy loss can be accepted. In return, the system can run without adjustment, and with very nearly the same energetic cost, on most surfaces. The exceptions are very soft surfaces on which the foot sinks appreciably into the soil doing appreciable deformation work. Additional energy must be added to the system by the actuator.

Extending this to an idealized quadruped and ignoring the effects of rotation, the energy loss per stride in a pronk is $mg^2T^2/2$ where T is the stride duration. The corresponding loss per stride for a gait in which the feet are placed in pairs—trot, bound, or pace—is $mg^2T^2/8$, assuming that the stride period is equally divided. For an ideal gallop with the feet placed individually at equal intervals, it is $mg^2T^2/32$. These values serve as baselines for the magnitudes that might be expected from a more detailed analysis performed for bounding and galloping below. The actual values will be equal to, or larger than, these due to the effects of pitch and/or roll rotations and the uneven distribution of the footfalls over the stride period.

The energy that is lost in the impact of the foot with the ground appears to the system as an increase in the external drag, **D**. The way this works is somewhat analogous to the generation of rolling resistance at a wheel [10].

The dramatic decrease in impact energy losses when transitioning from a trot to a gallop provides part of the reason why animals transition to the gallop gait when moving fast enough to generate flight phases. However, the discussion so far ignores energy interchange between horizontal kinetic energy, vertical kinetic energy, gravitational potential energy, and internal energy losses. This interchange takes place during stance and is characterized by a horizontal deceleration at the beginning of stance followed by acceleration after the foot has passed under the hip/shoulder joint. In a fast gallop, the acceleration more or less completely balances the deceleration at the front legs [3], so the net horizontal velocity change over the front stance is zero. There is a net accelerative component from the back legs that is sufficient to overcome the effect of drag on the system. There is a considerable literature on internal energy storage during running, and the amount of energy stored as strain energy, as opposed to gravitational potential energy during stance [9,11–13]. This discussion is interesting and compatible with the models discussed here. It is important for a complete understanding of the gait mechanics. In the present paper we try to focus on the rest of the story: the mechanics of the intervals between stances and the phasing of the stances. We assume that the internal energy losses are determined by the horizontal running speed and focus on the energy losses inherent in the interaction with the ground. According to the viewpoint used here, the spring serves to dynamically isolate the foot from the rest of the system. Its primary effect is to extend the duration of the stance phase beyond the instantaneous contact one would get with a perfectly rigid ending on the leg. The spring stiffness, together with M, determines the duration of stance [15,16].

The mechanics of the system during stance is often considered to follow the SLIP (single leg inverted pendulum) model. This has been extensively studied, and its properties are well understood [12,14]. The principal implication for the present purpose is that the upward vertical velocity component immediately after stance is exactly equal in magnitude to the downward vertical velocity immediately before stance. We will show that this condition is excessively restrictive and that the SLIP model is not, in general, consistent with a bound and cannot be consistent with a three-dimensional gallop.

It is a property of a ballistic trajectory that the duration of each hop is directly proportional to the vertical velocity at lift-off. Since the energy lost to impact when placing a foot is directly proportional to the square of the vertical velocity of the system at impact, the peak height of the hop is proportional to the square of the vertical velocity at lift-off. An observation of animals running shows that their stride frequency increases only slowly with speed. In fact, one might hypothesize that the observed increase in stride frequency is a result of the necessary decrease in stance duration with speed, and that the effective duration of the ballistic trajectory is constant.

Hence, the duration of each hop is approximately constant, indicating that the vertical velocity at lift-off is approximately constant, and hence the height of each hop is also constant. Since the number of footfalls/s is approximately constant, the rate of energy loss due to the foot impacts is approximately constant. The increase in energy cost with increasing speed is largely due to increasing external drag and internal losses. This is consistent with our observations running the KOLT (kinematically ordered locomotive tetrapod) machine shown in Fig. 4 [15,16]. This model, which will be used to estimate the relative energy losses of bound, trot, and gallop gaits, has a lot in common with the "rimless wheel" model [17]. It is apparent that the least loss of energy per stride due to the vertical impact is obtained by spacing the footfalls evenly throughout the stride period. However, this even spacing is inconsistent with the dynamic interaction between the bal-

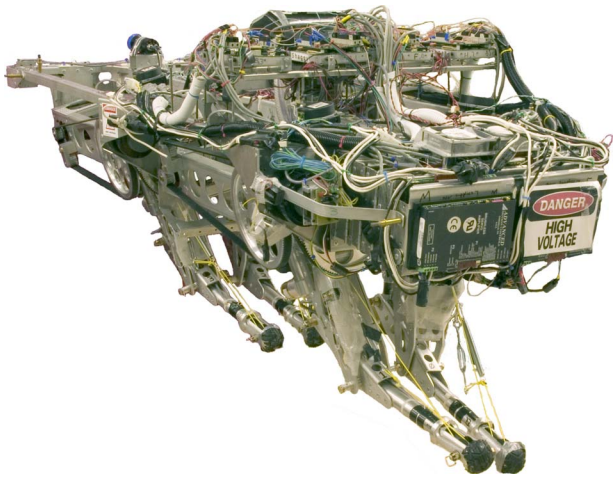

Fig. 4 The KOLT running machine that is in operation in the Stanford Robotic Locomotion Laboratory

listic saccades of the center of mass and the constant velocity rotations required by the conservation of angular momentum. Considering a bound and observing that the impact energy loss is proportional to the sum of the increases in the height of the center of mass during the two hops, it follows that the energy loss is minimized when the two hops have equal heights and hence equal durations.

We recall that the impulsive moment balance (Eq. (3) above) requires that the ratio of the magnitudes of the vertical impulses of the front and rear feet be b/a. Considering the vertical motion of the center of mass, the ratio of the duration of the hop off the front feet to that off the rear feet would also be b/a, so it would appear that the durations of the hops cannot be equal.

Bounding

Let the vertical velocity of the center of mass of the system immediately before the front foot impact be u_F, regarded as being positive in the upward direction, and that immediately after the impact be u'_F. The vertical velocity immediately before the rear foot impact is u_R, and that immediately after is u'_R. If the vertical impulse delivered by a front foot is J_{zF} and that delivered by a rear foot is J_{zR}, then applying impulse-momentum across the impacts gives

$$u'_F = u_F + \frac{2J_{zF}}{M}, \quad u'_R = u_R + \frac{2J_{zR}}{M}, \quad \omega_{yFR} = \omega_{yRF} - \frac{2aJ_{zF}}{I_y} \tag{5}$$

where ω_{yFR} is the pitch angular velocity after the front foot stance and before the rear foot stance, and ω_{yRF} is the corresponding angular velocity after the rear foot stance.

Looking at the velocity changes during the two ballistic trajectories (hops),

$$u_R = u'_F - g\tau_{FR}, \quad u_F = u'_R - g\tau_{RF} \tag{6}$$

Here τ_{FR} is the time period from the front foot stance to the rear foot stance, and τ_{RF} is that between the rear stance and the front. Obviously

$$\tau_{FR} + \tau_{RF} = T \tag{7}$$

where T is the stride period.

Applying the condition that the vertical height of the center of mass at the end of the stride must be identical with that at the beginning,

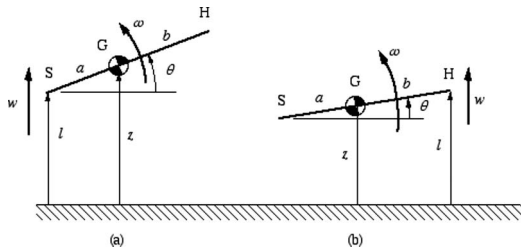

Fig. 5 Coordinate senses during the (*a*) front foot stance, and (*b*) rear foot stance. Point S represents the shoulder joint, and point H represents the hip joint. G is the center of mass.

$$(u'_F + u_R)\tau_{FR} + (u'_R + u_F)\tau_{RF} = 0 \tag{8}$$

where M is the total mass of the system and I_y is its pitch moment of inertia about G. J_{Fz} is the vertical component of the impulse delivered by each front foot.

The condition that the system must return to the same pitch angle after a complete stride gives

$$\omega_{yFR}\tau_{FR} + \omega_{yRF}\tau_{RF} = 0 \tag{9}$$

Combining Eqs. (5), (6), and (8) gives

$$u'_F = \frac{gT}{2(a+b)}(2ap - a + b), \quad u'_R = \frac{gT}{2(a+b)}(b + a - 2bp)$$
$$u_F = \frac{gT}{2(a+b)}(2ap - a - b), \quad u_R = \frac{gT}{2(a+b)}(b - a - 2bp) \tag{10}$$

Here $p = \tau_{FR}/T$ and $1-p = \tau_{RF}/T$.

Note that we can apply Eqs. (2) and (3) above to get

$$J_{Fz} = \frac{bMgT}{2(a+b)}, \quad J_{Rz} = \frac{aMgT}{2(a+b)} \tag{11}$$

These expressions are also used in the derivation of Eq. (10) above. Similarly, Eqs. (5) and (9) can be combined to give

$$\omega_{yFR} = \frac{\kappa gT}{a+b}(p-1), \quad \omega_{yRF} = \frac{\kappa gT}{a+b}p \tag{12}$$

where

$$\kappa = \frac{Mab}{I_y} \tag{13}$$

The parameter κ actually measures the relative magnitudes of the impulsive moment about the pitch axis and the impulse of the inertial moment about that axis. Thus, it quantifies the importance of pitch rotation in the model.

Energy Loss. We will use the energy loss due to the impact of the feet with the ground to estimate the optimal value of p and hence the optimal time division between the two ballistic saccades that make up the stride.

The velocity, w_F, with which the front feet strike the ground may be obtained from Eq. (10) with reference to Fig. 5,

$$w_F = -u_F + a\omega_{yRF} = \frac{gT}{2}\left(1 - \frac{2ap(1-\kappa)}{a+b}\right)$$
$$w_R = -u_R - b\omega_{yFR} = \frac{gT}{2}\left(1 - \frac{2b(1-p)(1-\kappa)}{a+b}\right) \tag{14}$$

The energy lost in each stride due to impact with the ground is

$$U_L = m_F w_F^2 + m_R w_R^2 \tag{15}$$

Differentiation with respect to p to find the extremal value of U_L gives

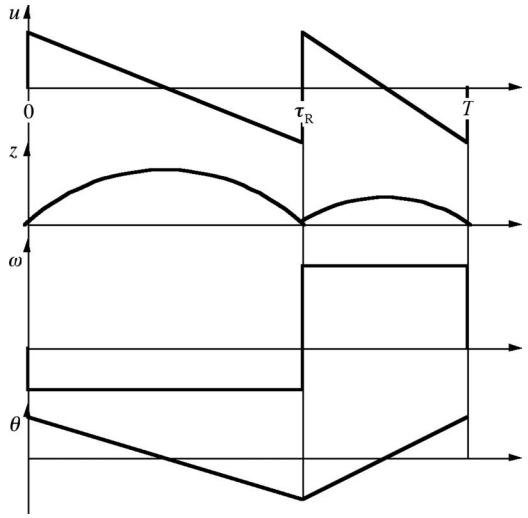

Fig. 6 Variations in vertical velocity and vertical position of center of mass, and pitch angular velocity and pitch angle through a bound stride. The intervals used in the text are $\tau_{FR} = \tau_R$ and $\tau_{RF} = T - \tau_R$.

$$p = \frac{m_F a(a+b) - m_R b(a - b(1-2\kappa))}{2(1-\kappa)(m_F a^2 + m_R b^2)} \tag{16}$$

as the value of p that extremizes the energy consumption. The corresponding value of U_L is given by

$$U_L = \frac{g^2 T^2 m_F m_R (a^2 + b^2 + 2ab\kappa)^2}{4(a+b)^2(a^2 m_F + b^2 m_R)} \tag{17}$$

It is easily shown that d^2U_L/dp^2 has the form of a sum of two squares and is hence always positive, thereby establishing that the value of U_L given by Eq. (17) is the minimum value. This might be compared with the corresponding values for a trot,

$$U_L = \frac{g^2 T^2}{16}(m_F + m_R) \tag{18}$$

The impact energy cost for trotting is, in fact, the same as that of the idealized two foot gait quoted above because p is constrained to be 0.5 by the symmetry of the gait, and there is no body rotation. The ratio of the values given by Eqs. (17) and (18) is

$$\frac{U_{L\ \text{bound}}}{U_{L\ \text{ideal}}} = \frac{4m_F m_R (a^2 + b^2 + 2ab\kappa)^2}{(a+b)^2(a^2 m_F + b^2 m_R)(m_F + m_R)} \tag{19}$$

This ratio is always greater than 1 indicating that the energy loss for the bound is always greater than that for the trot. This is best seen by setting $a=b$, assuming that the effective masses of the front and rear feet are equal $m_F=m_R=m$, and substituting in Eq. (19). There is always a term which is a function of κ that increases the energy loss for the bound. κ expresses the effect of body rotation in a bound. Figure 6 shows the variations in vertical velocity and height of the center of mass, and the pitch angular velocity and attitude through the bound stride.

Galloping

Approach. We follow the suggestion of Minetti [18] and regard the gallop as a bound in which the front and rear leg pairs "skip." The advantage of splitting out the legs at each stance becomes obvious if we recall that the impulse impelling each hop is halved. Based on the discussion above, to a first approximation this means that the energy going into a vertical motion in each hop is one-eighth of that for the hops in a bound, taking into account that two feet impact at the end of each hop in a bound. However, since there are four hops rather than two, the energy loss in a gallop should be approximately one-quarter of that in a bound.

We can regard a gallop as being an asymmetric bound in which the front and rear leg pairs skip. That is, we start with a bound and examine the effects of separating the front feet and the back feet. Instead of placing the front feet together, we place foot 1 ahead of foot 2. For a transverse gallop, we would then place foot 3 ahead of foot 4. The hops *FR* and *RF* of the bound correspond to flight phases 23 and 41 of the gallop, while the skips are hops 12 and 34.

The stride cycle impulse-momentum relationships are still satisfied. The separation of the two front foot impulses does not affect Eqs. (1)–(3) above. Likewise, the relationship between the angular velocities $\omega_{y23} = \omega_{yFR}$ and $\omega_{y41} = \omega_{yRF}$ remain the same. The change in angular velocity occurs in two steps instead of one.

Using a notation similar to that above and applying linear and angular momentum balances across the stance of leg 1,

$$Mu_1 + J_{Fz} = Mu_1', \quad I_y\omega_{y41} - aJ_{Fz} = I_y\omega_{y12}, \quad I_x\omega_{x41} + cJ_{Fz} = I_x\omega_{x12}$$

Hence, applying the corresponding relationships to the other stances,

$$u_1' = u_1 + \frac{J_{zF}}{M}, \quad u_2' = u_2 + \frac{J_{zF}}{M}, \quad u_3' = u_3 + \frac{J_{zR}}{M}, \quad u_4' = u_4 + \frac{J_{zR}}{M} \tag{20}$$

$$\omega_{y12} = \omega_{y41} - \frac{aJ_{zF}}{I_y}, \quad \omega_{y23} = \omega_{y12} - \frac{aJ_{zF}}{I_y}$$
$$\omega_{y34} = \omega_{y23} + \frac{bJ_{zR}}{I_y}, \quad \omega_{y41} = \omega_{y34} + \frac{bJ_{zR}}{I_y} \tag{21}$$

$$\omega_{x12} = \omega_{x41} + \frac{cJ_{zF}}{I_x}, \quad \omega_{x23} = \omega_{x12} - \frac{cJ_{zF}}{I_x}$$
$$\omega_{x34} = \omega_{x23} + \frac{dJ_{zR}}{I_x}, \quad \omega_{x41} = \omega_{x34} - \frac{dJ_{zR}}{I_x} \tag{22}$$

Let the effective times of the impulse of foot 1 be 0 and T, where T is the stride period. Also let the effective times of the impulses for feet 2, 3, and 4 be τ_2, τ_3, and τ_4, respectively. It is convenient also to define symbols for the intervals between successive footfalls: $\tau_{12}=\tau_2$, $\tau_{23}=\tau_3-\tau_2$, $\tau_{34}=\tau_4-\tau_3$, and $\tau_{41}=T-\tau_4$. Then for the hops between impulses, we have

$$u_2 - u_1' = -g\tau_{12}, \quad u_3 - u_2' = -g\tau_{23}, \quad u_4 - u_3' = -g\tau_{34}$$
$$u_1 - u_4' = -g\tau_{41} \tag{23}$$

In a steadily repetitive cycle, the vertical position of the center of mass and the angular attitude at the end of the cycle should be the same as at those the beginning of the cycle. Hence

$$(u_1' + u_2)\tau_{12} + (u_2' + u_3)\tau_{23} + (u_3' + u_4)\tau_{34} + (u_4' + u_1)\tau_{41} = 0$$

$$\omega_{y12}\tau_{12} + \omega_{y23}\tau_{23} + \omega_{y34}\tau_{34} + \omega_{y41}\tau_{41} = 0 \tag{24}$$

$$\omega_{x12}\tau_{12} + \omega_{x23}\tau_{23} + \omega_{x34}\tau_{34} + \omega_{x41}\tau_{41} = 0$$

Combining the sets of Eqs. (20) and (22)–(24) and the expressions for the vertical impulses given by Eq. (11), we can express the vertical velocities in terms of τ_{12}, τ_{23}, τ_{34}, and τ_{41},

$$u_1' = \frac{g}{2(a+b)}\{(a+b)\tau_{12} + a(\tau_{23} - \tau_{41})\}$$

$$u_2 = \frac{g}{2(a+b)}\{-(a+b)\tau_{12} + a(\tau_{23} - \tau_{41})\}$$

$$u_2' = \frac{g}{2(a+b)}\{(a+b)\tau_{23} - a(\tau_{12} + \tau_{41}) + b(\tau_{41} + \tau_{34})\} \tag{25}$$

$$u_3 = \frac{g}{2(a+b)}\{-(a+b)\tau_{23} - a(\tau_{12} + \tau_{41}) + b(\tau_{41} + \tau_{34})\}$$

$$u_3' = \frac{g}{2(a+b)}\{(a+b)\tau_{34} + b(\tau_{41} - \tau_{23})\}$$

$$u_4 = \frac{g}{2(a+b)}\{-(a+b)\tau_{34} + b(\tau_{41} - \tau_{23})\} \tag{26}$$

$$u_4' = \frac{g}{2(a+b)}\{(a+b)\tau_{41} + a(\tau_{12} + \tau_{23}) - b(\tau_{23} + \tau_{34})\}$$

$$u_1 = \frac{g}{2(a+b)}\{-(a+b)\tau_{41} + a(\tau_{12} + \tau_{23}) - b(\tau_{23} + \tau_{34})\}$$

Similarly, for the angular velocities

$$\omega_{y12} = \frac{\kappa g}{2(a+b)}(\tau_{23} - \tau_{41}), \quad \omega_{y23} = \frac{\kappa g}{2(a+b)}(\tau_{23} - \tau_{41} - T) \tag{27}$$

$$\omega_{y34} = \omega_{y12}, \quad \omega_{y41} = \frac{\kappa g}{2(a+b)}(\tau_{23} - \tau_{41} + T)$$

At this point it is convenient to make the assumption that

$$\frac{c}{d} = \frac{a}{b} \tag{28}$$

This assumption greatly simplifies the mathematics. It is consistent with the condition for a passively stable trot [19]. It is also consistent with the common observation that in a biological gallop, the rear legs move outside the front legs to avoid interference. Hence the track of the rear feet tends to be wider than that of the front even though the width across the shoulders may be equal to or greater than that across the hips. There is, however, no empirical evidence either supporting the satisfaction of Eq. (28) or negating it. The effective values of c and d are easily adjusted regardless of the hip and shoulder widths by applying appropriate torques about the x direction at the hip and shoulder joints. This can be done passively by applying the appropriate muscles isometrically.

The system can be solved without making the assumption of Eq. (28), but the solution is more complex. If the assumption is made,

$$\omega_{x12} = \frac{\lambda g}{2(c+d)}(\tau_{23} + \tau_{41}), \quad \omega_{x23} = -\frac{\lambda g}{2(c+d)}(\tau_{12} + \tau_{34}) \tag{29}$$

$$\omega_{x34} = \omega_{x12}, \quad \omega_{x41} = \omega_{x23}$$

where

$$\lambda = \frac{Mcd}{I_x} \tag{30}$$

The parameter λ quantifies the effects of rotation about the roll axis in the same way that κ expresses those about the pitch axis.

In addition to the condition that the center of mass must be at the same height above the ground at the beginning and end of a full stride, we assume that the left-right leg pairs operate at the same working heights. This condition yields, in principle, three more vertical displacement equations, in addition to the first of Eq. (24). However, two of these yield only expressions for the initial attitude angles θ_{y1} and θ_{x1}. Applying this condition to the front and rear leg pairs, respectively, we have

$$(l + a\theta_{y2} + c\theta_{x2}) - (l + a\theta_{y1} - c\theta_{x1}) = \frac{u_1' + u_2}{2}\tau_{12}$$

$$(l - b\theta_{y4} + d\theta_{x4}) - (l - b\theta_{y3} - d\theta_{x3}) = \frac{u_3' + u_4}{2}\tau_{34}$$

giving

$$a\omega_{y12}\tau_{12} + c(2\theta_{x1} + \omega_{x12}\tau_{12}) = \frac{ga}{2(a+b)}(\tau_{23} - \tau_{41})\tau_{12}$$

$$-b\omega_{y34}\tau_{34} + d(2\theta_{x3} + \omega_{x34}\tau_{34}) = \frac{gb}{2(a+b)}(\tau_{41} - \tau_{23})\tau_{34}$$

Since

$$\theta_{x3} = \theta_{x1} + \omega_{x12}\tau_{12} + \omega_{x23}\tau_{23} = \theta_{x1} + \frac{\lambda g}{2(c+d)}(\tau_{41}\tau_{12} - \tau_{34}\tau_{23})$$

we can eliminate θ_{x1} to give, after simplification,

$$(1 - \kappa - \lambda)(\tau_{12} + \tau_{34})(\tau_{23} - \tau_{41}) = 0 \tag{31}$$

Since, in general, $1 - \kappa - \lambda \neq 0$, either

$$\tau_{23} = \tau_{41} \quad \text{or} \quad \tau_{12} + \tau_{34} = 0 \tag{32}$$

The second of Eq. (32) implies $\tau_{12} = \tau_{43}$. That is, the order of stances 3 and 4 is reversed into the sequence of a rotary gallop. The rotary gallop case will be discussed in detail via a separate development below.

Hence the only solution consistent with a transverse gallop is that the two flight-phase durations are equal, and the skip durations τ_{12} and τ_{34} are not constrained. This is a surprise since the bound solution allowed unequal values of τ_{FR} and τ_{RF} that respectively correspond to τ_{23} and τ_{41}.

Substitution back into Eqs. (25)–(27) gives

$$u_1' = \frac{gTp}{2}, \quad u_2 = -\frac{gTp}{2}$$

$$u_2' = \frac{gT}{2}\left(-p + \frac{b}{a+b}\right), \quad u_3 = \frac{gT}{2}\left(q - \frac{a}{a+b}\right) \tag{33}$$

$$u_3' = \frac{gTq}{2}, \quad u_4 = -\frac{gTq}{2}$$

$$u_4' = \frac{gT}{2}\left(-q + \frac{a}{a+b}\right), \quad u_1 = \frac{gT}{2}\left(p - \frac{b}{a+b}\right)$$

where

$$p = \frac{\tau_{12}}{T}, \quad q = \frac{\tau_{34}}{T}$$

Similarly

$$\omega_{y12} = 0, \quad \omega_{y23} = -\frac{\kappa gT}{2(a+b)}, \quad \omega_{y34} = 0, \quad \omega_{y41} = \frac{\kappa gT}{2(a+b)}$$

$$\omega_{x12} = \frac{\lambda gT(1-p-q)}{2(c+d)}, \quad \omega_{x23} = -\frac{\lambda gT(p+q)}{2(c+d)} \tag{34}$$

$$\omega_{x34} = \omega_{x12}, \quad \omega_{x41} = \omega_{x23}$$

On the face of it, this solution, with the flight phases being of equal durations, is not consistent with the apparent asymmetry of the gait. It is a basic feature of the gallop that the gathered flight

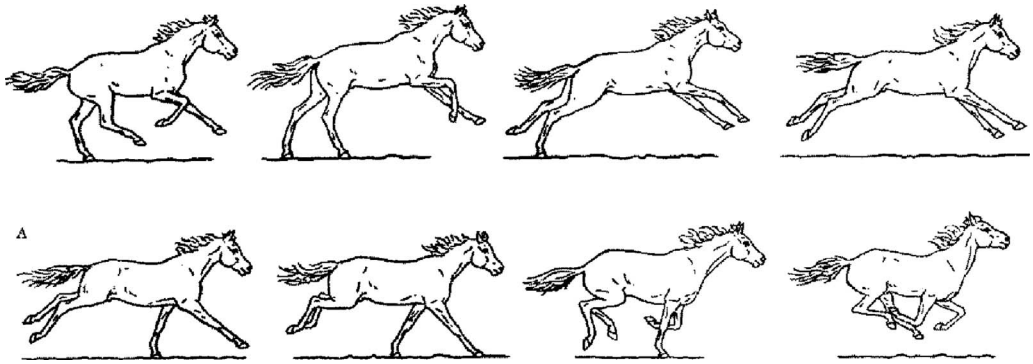

Fig. 7 Fast gallop of a horse reproduced from Gambaryan [8]. The right-hand frame in the top row is the spread flight phase. The corresponding frame in the bottom row is the gathered flight phase.

phase (Eq. (23)) is always present, but the spread flight phase (Eq. (43)) is only present in a fast gallop and then appears to be significantly shorter than the gathered flight phase.

There is an explanation, if we recall, that our model treats the stances as impulsive events. In fact, the stances are of duration comparable to the foot placement intervals, and there are no "flight phases" between the footfalls of the front legs or the rear legs. Rather, there are periods of double support. This does not negate the validity of the impulsive model, but it is necessary to interpret it in the light of the actual durations of the stances. The effect is to shorten the apparent durations of the gathered and spread flight phases and, in fact, to disproportionately shorten the apparent duration of the spread flight phase.

A second consideration is that we have assumed, for convenience, that the principal moments of inertia and, consequently, κ and λ are constant. However, we know from Ref. [4] that the pitch moment of inertia, and hence κ, varies by about one-third between the gathered and spread flight phases and the roll moment of inertia, and hence λ varies by a factor of 2. While λ is small and its variation is probably not significant, the variation of κ can certainly be expected to affect the durations of the flight phases. A more detailed model incorporating the variations of the inertia moments and fully modeling the durations of the stances may resolve this apparent paradox .

When viewed in the body reference frame, the impulses delivered by the legs are inclined, as illustrated in Fig. 1. As may be seen in Fig. 7, when viewed from a fixed frame, the front foot touches down far in front of the shoulder and lifts off a short distance behind the shoulder. The rear foot touches down almost directly beneath the hip and lifts off after the leg has extended far to the rear of the hip. The effect is to shorten or erase the period when all feet are physically out of contact with the ground when going from a rear foot stance to a front foot stance (Eq. (43)) and to emphasize the flight period when going from a front foot stance to a rear foot stance (Eq. (23)). Thus, the apparent asymmetry between the gathered flight phase (Eq. (23)) and the spread flight phase (Eq. (43)) as viewed in a fixed reference frame, as opposed to the body reference frame used for our analysis, is not necessarily inconsistent with equal values of τ_{23} and τ_{41}, although it would certainly be of value to run an experiment in which sufficient data were collected to verify or negate the result. A further observation is that Fig. 7 is a set of tracings from frames of a high-speed movie and that an examination of the height of the body above the ground during the gathered and spread flight phases reveals that it may well be the same, as it would need to be if intervals (23) and (14) are equal. Again the eye tends to be misled by the positions of the legs that are folded under the body well clear of the ground during the gathered phase but are extended toward the ground, resulting in a small clearance during the spread phase.

It may be observed from Eq. (33) that $u_2'=-u_1$, $u_2=-u_1'$, $u_4'=-u_3$, $u_4=-u_3'$. Further, since $w_1=u_1-a\omega_{y41}+c\omega_{x41}$, etc., applying the solutions of Eq. (34) leads to $w_2'=-w_1$, $w_2=-w_1'$, $w_4'=-w_3$, and $w_4=-w_3'$, but, in general, $w_1'\neq -w_1$, $w_2'\neq -w_2$, $w_3'\neq -w_3$, and $w_4'\neq -w_4$. The inequalities of the magnitudes of the velocities of the feet before and after each impact violate the SLIP model. Rather, we see that the magnitude of the velocity with which the *first* foot impacts in each SLIP combination is equal to the velocity with which the *second* foot leaves the ground. Similarly, the magnitude of the velocity with which the second foot impacts is the same as that with which the first leaves the ground. The impact velocity of the second foot is substantially lower than that of the first foot. This is consistent with the observations in Ref. [3] and those that show that the first foot to impact before each double stance does so at higher velocity than the second. However, in Ref. [3] it is also observed that despite this the resultant impulses generated by the feet in each pair were almost identical.

Longitudinal Motion. Longitudinal motion is only loosely coupled to the motion in the vertical direction and associated pitch and roll. We have the following relationships for the forward (x) velocities of the center of mass:

$$v_1'=v_1+\frac{J_{xF}}{M},\quad v_2'=v_2+\frac{J_{xF}}{M},\quad v_3'=v_3+\frac{J_{xR}}{M},\quad v_4'=v_4+\frac{J_{xR}}{M}$$

$$v_2=v_1'-\frac{D\tau_{12}}{M},\quad v_3=v_2'-\frac{D\tau_{23}}{M},\quad v_4=v_3'-\frac{D\tau_{34}}{M} \tag{35}$$

$$v_1=v_4'-\frac{D\tau_{41}}{M}$$

Now the individual placement of the feet and the lateral distances between the feet result in impulsive moments about the yaw (z) axis, so we have nonzero yaw angular velocities,

$$\omega_{z12}=\omega_{z41}-\frac{cJ_{xF}}{I_z},\quad \omega_{z23}=\omega_{z12}+\frac{cJ_{xF}}{I_z}$$

$$\omega_{z34}=\omega_{z23}-\frac{dJ_{xF}}{I_z},\quad \omega_{z41}=\omega_{z34}+\frac{dJ_{xF}}{I_z} \tag{36}$$

We can relate the longitudinal velocities of the center of mass to the average velocity of the center of mass over the complete stride

$$VT=\left(\frac{v_1'+v_2}{2}\right)\tau_{12}+\left(\frac{v_2'+v_3}{2}\right)\tau_{23}+\left(\frac{v_3'+v_4}{2}\right)\tau_{34}+\left(\frac{v_4'+v_1}{2}\right)\tau_{41} \tag{37}$$

Combining Eqs. (35) and (37) gives

$$
\begin{aligned}
v_1' &= V + \frac{DT}{2M}p, \quad v_1 = V + \frac{DT}{2M}p - \frac{J_{xF}}{M} \\
v_2' &= V - \frac{DT}{2M}p + \frac{J_{xF}}{M}, \quad v_2 = V - \frac{DT}{2M}p \\
v_3' &= V + \frac{DT}{2M}q, \quad v_3 = V + \frac{DT}{2M}q - \frac{J_{xR}}{M} \\
v_4' &= V - \frac{DT}{2M}q + \frac{J_{xR}}{M}, \quad v_4 = V - \frac{DT}{2M}q
\end{aligned}
\tag{38}
$$

Eq. (38) provides a time history of the forward velocity of the center of mass over the course of a stride. Also, over the complete stride the yaw angles must sum to zero,

$$\omega_{z12}\tau_{12} + \omega_{z23}\tau_{23} + \omega_{z34}\tau_{34} + \omega_{z41}\tau_{41} = 0 \tag{39}$$

Equations (35) and (38) lead to

$$
\begin{aligned}
\omega_{z12} &= \frac{1}{I_z}\{dJ_{xR}q - cJ_{xF}(1-p+q)\} \\
\omega_{z34} &= \frac{1}{I_z}\{dJ_{xR}(q-1) + cJ_{xF}(p-q)\} \\
\omega_{z23} &= \omega_{z41} = \frac{1}{I_z}\{dJ_{xR}q + cJ_{xF}(p-q)\}
\end{aligned}
\tag{40}
$$

Equation (40) describes the yaw angular velocity changes through the stride. Based on Eqs. (38) and (40), we can plot time histories of longitudinal velocity and displacement of the center of mass, and yaw angular velocity and displacement to complement Fig. 8, which gives the corresponding information for vertical displacement and pitch and roll rotation.

Energy Loss. The vertical velocity of the foot immediately before impact with the ground at stance 1 is

$$w_1 = u_1 - a\omega_{y41} + c\omega_{x41}$$

Substitution from Eqs. (33) and (34) gives the following expressions for the vertical velocities of the feet immediately before impact

$$
\begin{aligned}
w_1 &= \frac{gT}{2(a+b)}\{(a+b)p + b + \kappa a + \lambda a(p+q)\} \\
w_2 &= \frac{gT}{2(a+b)}\{(a+b)p + \lambda a(1-p-q)\} \\
w_3 &= \frac{gT}{2(a+b)}\{(a+b)q + a + \kappa b + \lambda b(p+q)\} \\
w_4 &= \frac{gT}{2(a+b)}\{(a+b)q + \lambda b(1-p-q)\}
\end{aligned}
\tag{41}
$$

The energy lost due to impacts in the gallop is

$$U_L = \frac{m_F}{2}(w_1^2 + w_2^2) + \frac{m_R}{2}(w_3^2 + w_4^2)$$

The conditions for an extremal value of U_L give

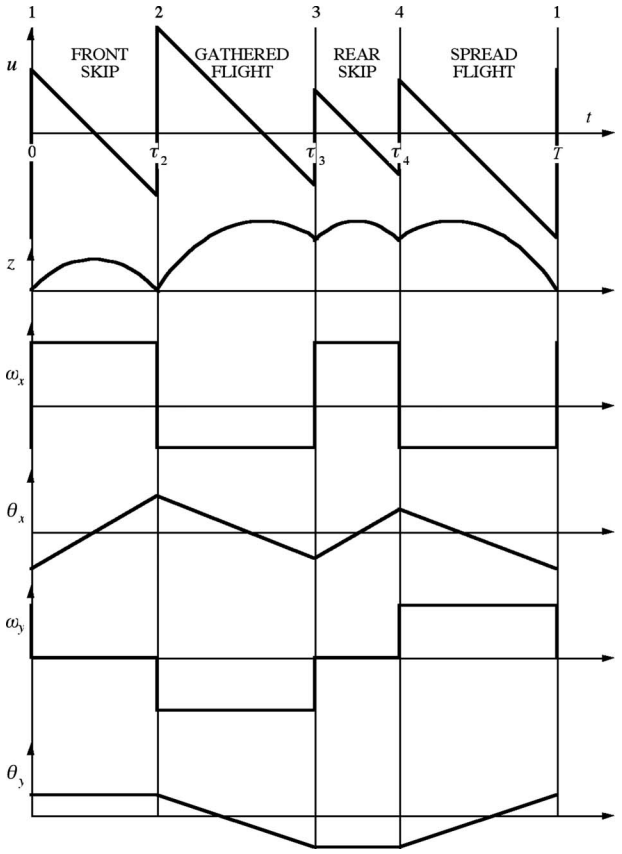

Fig. 8 Graphical presentation of variations of velocity and position variables through the transverse gallop stride

$$
\begin{aligned}
&p[m_F(a+b-\lambda a)^2 + m_R\lambda^2 b^2] - q[m_F\lambda a(a+b-\lambda a) \\
&\quad + m_R\lambda b(a+b-\lambda b)] \\
&\quad = \frac{1}{2}[m_F(b+(\kappa-\lambda)a)(a+b-\lambda a) - m_R\lambda b(a+(\kappa-\lambda)b)]
\end{aligned}
\tag{42}
$$

and

$$
\begin{aligned}
&p[m_F\lambda a(a+b-\lambda a) + m_R\lambda b(a+b-\lambda b)] \\
&\quad - q[m_F\lambda^2 a^2 + m_R(a+b-\lambda b)^2] \\
&\quad = \frac{1}{2}[m_F\lambda a(b+(\kappa-\lambda)a) - m_R(a+(\kappa-\lambda)b)(a+b-\lambda b)]
\end{aligned}
\tag{43}
$$

The solution for p and q gives

$$p = \frac{a\kappa + b(1-\lambda)}{2(a+b)(1-\lambda)}, \quad q = \frac{a(1-\lambda) + b\kappa}{2(a+b)(1-\lambda)} \tag{44}$$

Notice that the effective masses of the front and rear feet (m_F and m_R) cancel in these expressions, so the values of p and q given by Eq. (43) are independent of m_F and m_R. It is easily confirmed that these expressions for p and q minimize U_L. The minimal value is

$$U_L = \frac{g^2T^2}{16(a+b)^2}(m_F(a(\kappa+\lambda)+b)^2 + m_R(a+b(\kappa+\lambda))^2) \tag{45}$$

Therefore, the time intervals for the transverse gallop that minimize energy loss due to impact are

$$\tau_{12} = \frac{a\kappa + b(1-\lambda)}{2(a+b)(1-\lambda)}T, \quad \tau_{34} = \frac{a(1-\lambda) + b\kappa}{2(a+b)(1-\lambda)}T$$

$$\tau_{23} = \tau_{41} = \frac{1-\kappa-\lambda}{4(1-\lambda)}T \tag{46}$$

The ratio of the energy per stride lost to impact to the corresponding value for an ideal system with equally spaced footfalls and no body rotation is given by

$$\frac{U_{L\ \text{gallop}}}{U_{L\ \text{ideal}}} = \frac{4(m_F(a(\kappa+\lambda)+b)^2 + m_R(a+b(\kappa+\lambda))^2)}{(m_F+m_R)(a+b)^2} \tag{47}$$

This ratio is always greater than 1. It provides a measure of the importance of the rotational inertias and the location of the center of mass in determining the impact energy losses when galloping.

It may be noticed that Eq. (43) gives an energy loss rate that is constant or actually declines a little with speed since T declines slowly with speed. However, once again, these are only the losses associated with the interaction with the environment via the impacts between the feet and the ground. The internal losses that certainly increase with speed and air drag are not modeled here. Internal losses are estimated in stance phase models [9,14,17].

Discussion. It may be observed from Eq. (46) that the optimal durations τ_{23} and τ_{41} of the flight phases are functions solely of the inertial constants $\kappa = Mab/I_y$ and $\lambda = Mcd/I_x$. Also, since $\kappa < 1$ for galloping mammals and λ is typically an order of magnitude smaller than κ, $b > a$ implies that $\tau_{12} > \tau_{34}$. This is consistent with the observation that galloping mammals split their front feet further apart than their rear feet. Based on the data of Ref. [4], κ for the dog measured was 0.44, while λ was approximately 0.07. Using Eq. (45), these values give the energy optimal values $\tau_{12} = 0.41T$, $\tau_{34} = 0.33T$, and $\tau_{23} = \tau_{41} = 0.13T$.

The last of Eq. (45) implies that if $\kappa + \lambda > 1$, an energy optimal gallop is no longer possible. Even short of this, the durations of the flight phases are proportional to $1-\kappa-\lambda$. Since very fast runners use long flight phases, it is reasonable to conclude that increasing I_x and, particularly, I_y allows better use of the gallop gait. This may be another reason that many animals favor a posture with the head and neck extended well forward of the shoulders when running fast. It has the effect of increasing I_y.

Equation (47) may be compared to the corresponding expressions for the bound given by Eq. (19) above. We speculate that animals that are adapted to galloping for long distances likely have more mass distributed outside the shoulder-hip interval, mostly in the form of head and neck mass, and consequently have centers of mass close to the shoulders. Animals that are adapted for sprinting or for maneuverability may have more neutral weight distribution.

Equation (46) is a little surprising since the resulting durations of the flight phases are less than one-quarter of the stride period and are shorter than at least one of the skip periods. As was noted above, animals do not increase speed by increasing stride frequency. The stride period, T, declines only slowly with increasing speed. Rather, they increase speed by increasing the distance covered during each stride, particularly by increasing the durations of the flight phases. Although we do not model the stance phase in this paper, we hypothesize that the decrease in T is due to the decreasing durations of the stance phases. The duration of a stance phase depends on the angle through which the leg moves relative to the body while the foot is on the ground. It appears that this angle does not change much with changes in horizontal velocity. Hence, the duration of the stance phase is inversely proportional to horizontal velocity. This is certainly consistent with KOLT data. If the durations of the flight phases remain constant due to the maintenance of constant upward velocities of the center of mass at lift-off, the overall stride duration will decline slowly due to the shortened durations of the stances.

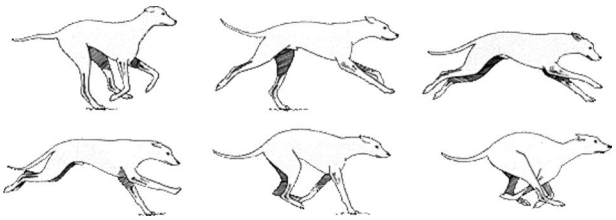

Fig. 9 Stances and spread and gathered flight phases of a rotary gallop as performed by a greyhound

Nevertheless, a fast gallop is dominated by long flight phases. It is apparent that the flight phases are extended at the cost of some increase in the energy lost to impact. Since impact energy losses become progressively less important than internal losses with increasing speed, nonoptimality is unlikely to be important.

In order to study this, we need to parametrize in a somewhat different way. First, we note that the distance between the feet during double stance along the line of motion cannot increase in proportion to the speed. Such an increase would rapidly exceed what is physically possible given the structure of the animal. Rather, we hypothesize that the distance the legs are split in the direction of motion during each skip remains constant, regardless of speed. This is generally consistent with observations via high-speed photography. This means that the durations of the skip intervals must decrease inversely with speed, thereby allowing the flight phases to occupy an increasing fraction of the overall stride period.

Rotary Gallop. The sequence of stances and flight phases for a rotary gallop as performed by a greyhound is shown in Fig. 9. As compared to Fig. 7, in which the horse places both rear and front feet in the left-right order, it may be observed that the dog places its rear feet in the right-left order and its front feet in the left-right order.

Here the footfall order is 1, 2, 4, 3. Following a development exactly analogous to that laid out above for a transverse gallop, and using the same notation, we get the following expression constraining the double stance and flight phase durations:

$$(1-\kappa-\lambda)(\tau_{12}-\tau_{43})(\tau_{24}-\tau_{31}) = 0 \tag{48}$$

As compared to the corresponding equation for the transverse gallop (Eq. (29)), we see that we have two possible solutions. As for the transverse gallop, one solution equates the flight phase durations

$$\tau_{24} = \tau_{31} \tag{49}$$

The other solution is, essentially, the same solution rotated at 90 deg. It equates the durations of the front and rear skips

$$\tau_{12} = \tau_{43} \tag{50}$$

This is a mathematically valid solution but is not physically viable for mammals.

Taking the solution given by Eq. (49) first and putting

$$p = \frac{\tau_{12}}{T}, \quad q = \frac{\tau_{43}}{T}, \quad \tau_{24} = \tau_{31} = \frac{T}{2}(1-p-q)$$

the velocity and angular velocity relationships become

$$u_1' = \frac{gTp}{2}, \quad u_2 = -\frac{gTp}{2}$$

$$u_2' = \frac{gT}{2}\left(-p + \frac{b}{a+b}\right), \quad u_4 = \frac{gT}{2}\left(q - \frac{a}{a+b}\right)$$

$$u_4' = \frac{gTq}{2}, \quad u_3 = -\frac{gTq}{2}$$

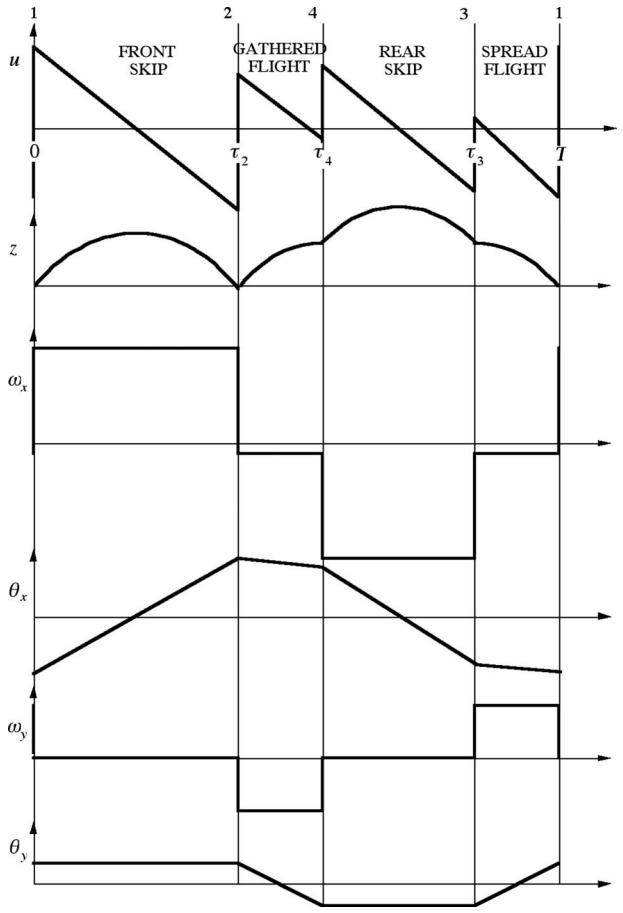

Fig. 10 Graphical representation of variations of position and velocity through a rotary gallop stride. This figure may be compared with the corresponding figure for a transverse gallop stride (Fig. 8). The most notable differences are in the roll (*x*) axis angular velocities and angular positions.

$$u_3' = \frac{gT}{2}\left(-q + \frac{a}{a+b}\right), \quad u_1 = \frac{gT}{2}\left(p - \frac{b}{a+b}\right) \tag{51}$$

and

$$\omega_{y12} = 0, \quad \omega_{y24} = -\frac{\kappa gT}{2(a+b)}, \quad \omega_{y43} = 0, \quad \omega_{y31} = \frac{\kappa gT}{2(a+b)}$$

$$\omega_{x12} = \frac{\lambda gT(1-p+q)}{2(c+d)}, \quad \omega_{x24} = \frac{\lambda gT(q-p)}{2(c+d)} \tag{52}$$

$$\omega_{x43} = -\frac{\lambda gT(1+p-q)}{2(c+d)}, \quad \omega_{x31} = \omega_{x24}$$

Using the same parameters as for the dog from Ref. [4], these equations give $\tau_{12}=0.39T$, $\tau_{12}=0.29T$, and $\tau_{24}=\tau_{31}=0.16T$. As may be seen, these values reflect a small increase in the durations of the flight phases as compared to the transverse gallop. Nevertheless, as previously noted, it is evident that animals extend the flight phases at the cost of optimality in order to run faster.

The variations in the velocities, angular velocities, vertical position, and angular attitude are shown schematically in Fig. 10. This may be compared with Fig. 8 for the transverse gallop. A notable difference is the relatively large roll excursions of the rotary gallop. This results from the feature of this gait of having a single roll oscillation in every stride, as compared to a double oscillation for the transverse gallop. It is apparent from high-speed photographs that some fast running animals that use rotary gallops exhibit large pelvic rotations, notably cheetahs. This may be an adaptation to reduce the effects of these large roll excursions.

Conclusions

The theory presented here predicts behaviors that resemble those observed in galloping mammals and also in robotic experiments in dynamic legged locomotion. However, it also raises many questions that will require more comprehensive measurements for their resolution.

In order to produce a mathematically workable and reasonably transparent model, we have made a number of assumptions about the system. Most of these can be shown to be approximately valid. However, the assumption that the principal moments of inertia of the system are aligned with the chosen body reference frame and are constant through the stride cycle is questionable. Also, there is an implicit assumption that the body is rigid. This runs counter to the observation that galloping mammals employ spinal flexure in the sagittal plane to lengthen their flight phases. This is evident in the extreme in cheetahs [8] but is a feature of galloping in all mammals. It does have the effect of changing the hip to shoulder distance and of varying the moments of inertia.

Notable results of this study include the following:

- discovery of the hidden symmetry in the gallop gait program embodied in the equality of the durations of the flight phases
- explanation of the differences between the impacts of the leading and trailing feet in each pair
- quantification of the expected skip intervals in terms of the system dimensions and inertial parameters
- explanation of several reasons why it is beneficial to a galloping system to have the center of mass closer to the shoulder than to the hips
- provision of a quantitative model of dynamic motions and energy losses external to the animal or a robot system that can be combined with a stance model to provide a complete, if simplified, dynamic model of the system
- validation of the results of the model by comparison with corresponding biological, robot, and simulation results, where available.

The results of this study also point out the importance of a comprehensive empirical observation of dynamic biological systems. It is necessary to combine force plate data, such as those presented in Ref. [3], with simultaneous calibrated high-speed video and with careful measurements of the kinematic structural features of the animal subjects. A methodology for doing this was provided in Ref. [4]. A photographic record or other means of plotting the positions of the footfalls of the running animal, both longitudinally and laterally, would be very valuable to confirm the theory as presented.

An alternative to the use of force plate data is the use of inertial sensors mounted on the body to estimate the changes in momentum and angular momentum resulting from the leg impulses [20]. This is similar to the localization of a dynamic robot using inertial sensing. It has the advantage of providing data continuously over an indefinite number of strides and does not require placement of the feet in specific locations, as is necessary for force plate readings.

Notable among the questions that need to be resolved or further explored are the issue of whether the observed difference in the duration of the gathered and spread flight phases can be adequately explained as an artifact of the finite durations of the stance phases and the differences in a model based on the body reference frame with observations in a fixed frame.

Another important question is: What actually limits the speed that a running system can attain? The answer to this from KOLT [16] is that as speed increases, the stance duration declines as the inverse of speed until the actuator can no longer deliver sufficient impulse in the time available. Thus, ultimately this is an actuation problem. One can speculate that a similar limitation applies to

biological systems. Certainly, available muscle force declines with the velocity of contraction as modeled by the well known Hill equation. Since impulse is, loosely, the product of the muscle force and the duration of action, the available impulse can be expected to drop sharply beyond a limiting stance duration. However, just as we do with KOLT, there is strong evidence that biological systems use elastic energy storage to circumvent the limitations of the primary actuator, so the question is, in fact, complex.

Acknowledgment

The authors acknowledge the support of the National Science Foundation, Grant Nos. IIS-0208664 and IIS-0535226, and the Secretaria de Estado de Universidades of the Spanish Ministry of Education and Science.

References

[1] Waldron, K. J., 2007, "A Coordination Scheme for an Asymmetrically Running Quadruped," *Proceedings of the IFToMM World Congress* (CD-ROM Proceedings), Besançon, France, Session No. RB-6, Paper No. 757.
[2] Krasny, D. P., and Orin, D. E., 2004, "Generating High-Speed Dynamic Running Gaits in a Quadruped Robot Using an Evolutionary Search," IEEE Trans. Syst., Man, Cybern., Part B: Cybern., **34**(4), pp. 1685–1696.
[3] Walter, R. M., and Carrier, D. R., 2007, "Ground Forces Applied by Galloping Dogs," J. Exp. Biol., **210**, pp. 208–216.
[4] Schmiedeler, J. P., Siston, R., and Waldron, K. J., 2002, "The Significance of Leg Mass in Modeling Quadrupedal Running Gaits," *ROMANSY 14: Theory and Practice of Robots and Manipulators*, G. Bianchi, J. C. Guinot, and C. Rzymkowski, eds., Springer, New York, pp. 481–488.
[5] Jayes, A. S., and Alexander, R. M., 1978, "Mechanics of Locomotion of Dogs and Sheep," J. Zool., **185**, pp. 289–308.
[6] Pandy, M. G., Kumar, V., Waldron, K. J., and Berme, N., 1988, "The Dynamics of Quadrupedal Locomotion," ASME J. Biomech. Eng., **110**(3), pp. 230–237.
[7] Alexander, R. McN., and Jayes, A. S., 1983, "A Dynamic Similarity Hypothesis for the Gaits of Quadrupedal Mammals," J. Zool., **201**, pp. 135–152.
[8] Gambaryan, P. P., 1974, *How Mammals Run: Anatomical Adaptions*, Wiley, New York.
[9] Abdallah, M. E., and Waldron, K. J., 2007, "Stiffness and Duty Factor Models for the Design of Running Bipeds," *Advances in Climbing and Walking Robots*, M. Xie, S. Dubowsky, J. G. Fontaine, M. O. Tokhi, and G. S. Virk, eds., World Scientific, Singapore, pp. 329–339.
[10] Schmiedeler, J. P., and Waldron, K. J., 1999, "The Effect of Drag on Gait Selection in Dynamic Quadrupedal Locomotion," Int. J. Robot. Res., **18**(12), pp. 1224–1234.
[11] Raibert, M. H., 1986, *Legged Robots That Balance*, MIT, Cambridge, MA.
[12] Saranli, U., Schwind, J., and Koditschek, D., 1998, "Toward the Control of a Multi-Jointed, Monopod Runner," *Proceedings of IEEE International Conference on Robotics and Automation*, Leuven, Belgium.
[13] Heglund, N. C., Cavagna, G. A., and Taylor, C. R., 1982, "Energetics and Mechanics of Locomotion III: Energy Changes of the Centre of Mass as a Function of Speed and Body Size in Birds and Mammals," J. Exp. Biol., **79**, pp. 41–56.
[14] Raibert, M. H., and Hodgins, J., 1991, "Animation of Dynamic Legged Locomotion," Comput. Graph., **25**, pp. 349–358.
[15] Estremera, J., and Waldron, K. J., 2006, "Leg Thrust Control for Stabilization of Dynamic Gaits in a Quadruped Robot," *Proceedings of ROMANSY 2006*, Warsaw, Poland, Jun. 20–22, pp. 213–220.
[16] Estremera, J., and Waldron, K. J., 2008, "Thrust Control, Stabilization and Energetics of a Quadruped Running Robot," Int. J. Robot. Res., in press.
[17] Ruina, A., Bertram, J. E. A., and Srinivasan, M., 2005, "A Collisional Model of the Energetic Cost of Support Work in Walking and Galloping, Pseudoelastic Leg Behavior in Running and the Walk-to-Run Transition," J. Theor. Biol., **237**, pp. 170–192.
[18] Minetti, A. E., 1998, "The Biomechanics of Skipping Gaits: A Third Locomotion Paradigm?," Proc. R. Soc. London, Ser. B, **265**, pp. 1227–1235.
[19] Waldron, K. J., and Kallem, V., 2004, "Control Modes for a Three-Dimensional Galloping Machine," *Proceedings of ASME Mechanisms Conference*, Paper No. DETC2004-57587.
[20] Singh, S., and Waldron, K., 2007, "Robotic Harness for the Field Assessment of Galloping Gaits," *Proceedings of the International Conference on Intelligent Robots and Systems (IROS)*, pp. 4247–2452.